2019 Rock Dynamics Summit– Aydan et al. (eds)
© 2019 Taylor & Francis Group, London, ISBN 978-0-367-34783-3

Centrifugal model tests on the seismic stability of rock foundations under critical facilities

A. Sekiguchi, M. Ishimaru, & T. Okada
Central Research Institute of Electric Power Industry, Chiba, Japan

K. Hiraga
CERES, Inc., Chiba, Japan

H. Morozumi
Kansai Electric Power Company, Inc., Osaka, Japan

ABSTRACT: In Japan, a slip safety factor based on an equivalent linear analysis is conventionally used to evaluate the stability of rock foundations under critical facilities in terms of the sliding motion during an earthquake. In this study, dynamic centrifugal model tests were performed to assess the seismic stability evaluation method for rock foundations. The results confirmed the feasibility of the method. In addition, the displacement of rock masses because of sliding was observed to be limited even when the slip safety factor had a value of less than 1. This confirms that, in the event of an earthquake, rock foundations do not become unstable spontaneously. Therefore, evaluating the seismic stability based on ground displacement is considered to be an effective approach.

1 INTRODUCTION

The occurrence of fatal and large-magnitude earthquakes in the recent past has increased attention on considering earthquake ground motions during the design phase of the construction of modern structures. Accordingly, the quantitative assessment of the seismic resistance of critical facilities to the earthquake-induced failure of rock foundations has become important.

In Japan, the seismic stability of rock foundations has conventionally been evaluated in terms of their bearing capacity, inclination, and sliding (JEAG 4601-1987 1987). With regard to the sliding motion during an earthquake, a slip safety factor based on an equivalent linear analysis is conventionally used to evaluate the stability of rock foundations. However, a slip safety factor value of less than 1 does not necessarily indicate immediate ground instability.

In this study, therefore, dynamic centrifugal model tests were performed to assess the applicability of conventional slip safety factor evaluation methods to the seismic stability of rock foundations.

2 CENTRIFUGAL MODEL TEST

A rock foundation model with a reduction ratio of 1:50 was constructed with artificial rock material and a weak layer. Vibration tests were performed in a centrifugal force field under a centrifugal acceleration of 50 g.

2.1 *Rock foundation model*

The rock foundation model and instrument arrangement are shown in Figure 1. The model was 200 mm (10 m upon real-scale conversion) in height and 300 mm in depth. The boundary surfaces had cutouts measuring 100 mm × 100 mm to avoid interference with the rigid box. The building model dimensions were 60 mm (width) × 40 mm (height) (3 m × 2 m upon real-scale conversion), and the density of the building material was 1200 kg/m^3.

The measured variables included accelerations produced under and on the ground surface along with the corresponding displacements induced in the building model and on the ground surface. A relative displacement gauge was installed at a position straddling the weak layer. For comparison, a second relative displacement gauge was installed on the ground surface immediately adjacent to the weak layer. Three pressure receiving plates were installed on the bottom of the building model, and the horizontal and vertical stresses were measured. The pressure receiving plates and ground surface were fixed with an adhesive.

2.2 *Properties of the rock foundation model*

Table 1 lists the physical properties of the materials used to construct the artificial rock model and weak layer. The properties were obtained from various physical and mechanical tests.

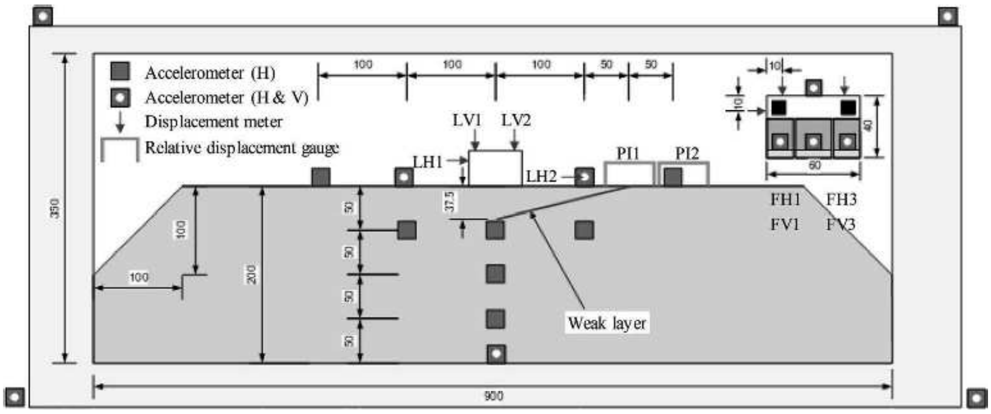

Figure 1. Rock foundation model and instrument arrangement.

Table 1. Physical properties of the artificial rock materials and weak layer (σm: mean stress).

	Rock	Weak layer
Unit weight	20.3 kN/m^3	20.6 kN/m^3
Peak shear strength	c_p = 267.1 kN/m^2 φ_p = 34.7°	c_p = 0.0 kN/m^2 φ_p = 28.6°
Residual shear strength	a = 4.61, b = 0.70 ($\tau_r = a \times \sigma_m{}^b$)	c_r = 0.0 kN/m^2 φ_r = 19.3°
Tensile strength	σ_t = 41.4 kN/m^2	σ_t = 0.0 kN/m^2
Initial elastic shear modulus	933000 kN/m^2	2800 kN/m^2
Poisson's ratio	0.42	0.49

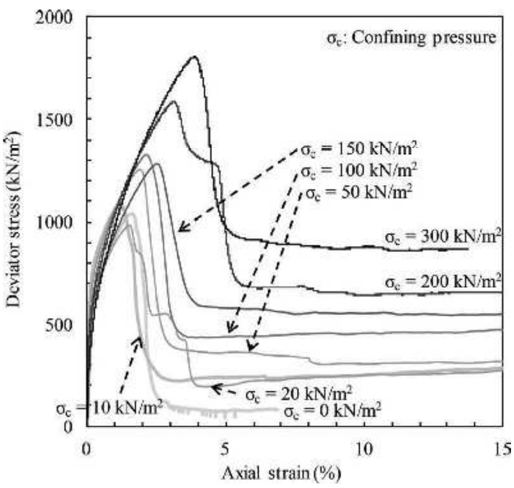

Figure 2. Stress–strain relationships obtained from plane-strain compression tests.

2.2.1 *Properties of the artificial rock materials*
Because the physical properties of different natural rocks vary considerably, the rock foundation model in this study was created from cement-modified soil with a curing period of 7 days. For a soil volume of approximately 1 m^3, the formulation was 82 kg of high early strength Portland cement, 370 kg of distilled water, 817 kg of crushed limestone sand, 817 kg of limestone fine powder, and 1 kg of admixture.

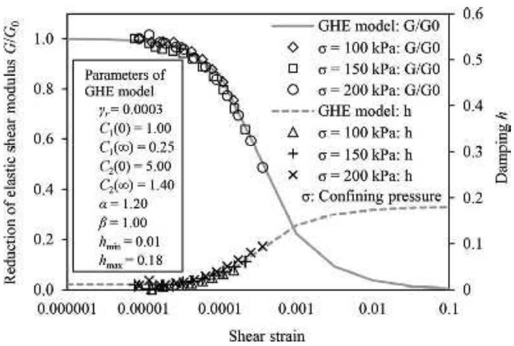

Figure 3. Dynamic deformation characteristics of the artificial rock material obtained from cyclic triaxial tests.

Figure 2 shows the stress–strain relationships obtained from plane-strain compression tests. Figure 3 shows the dynamic deformation characteristics obtained from cyclic triaxial tests.

2.2.2 *Properties of the artificial weak layer*
Based on the work by Ishimaru & Kawai (2011), the weak layer within the rock mass was reproduced by installing a 0.2 mm thick Teflon sheet within the rock foundation model before the artificial rock material started hardening. The resultant artificial weak layer had constant degrees of roughness, bite, etc. Prior examination confirmed that the cohesion between the post-hardening artificial rock material and Teflon sheet was very small. Under this condition, the shear resistance of the artificial weak layer can be considered to be equal to the frictional force generated between the artificial rock material and Teflon sheet.

The frictional force generated between the artificial rock material and Teflon sheet under normal-stress loading was examined through a

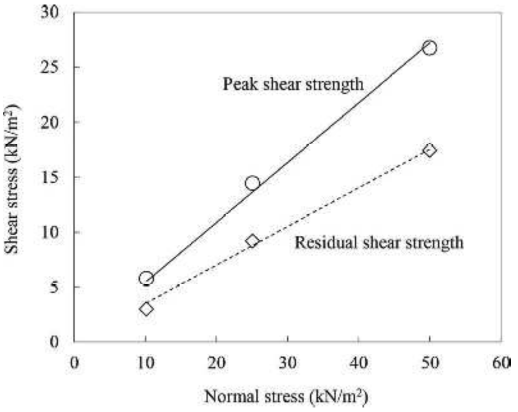

Figure 4. Shear stress–normal stress relationships obtained from single-plane shearing tests.

single-plane shearing test. Figure 4 shows the test results; the maximum and residual shear resistances increased in proportion to the normal stress.

2.3 *Input acceleration*

The input acceleration was provided in the form of a sinusoidal wave with a wavenumber of 20 (frequencies of 1.2 and 1.6 Hz upon real-scale conversion) in the main part with four tapers before and after. During the test, the acceleration amplitude was increased for each vibration step. A horizontal movement was the only input. However, the vertical motion, which was considered to be caused by the shaking table rocking, was also measured during vibration. Figure 5 shows the input acceleration of vibration step d04, and Table 2 lists the maximum acceleration amplitudes at different vibration steps. The 1.6-Hz excitation produced a greater vertical motion than the 1.2-Hz excitation owing to the characteristics of the experimental apparatus.

2.4 *Test results*

Figure 6 shows the maximum values during vibration and the accumulated residual values for the inclination of the building model at different vibration steps. The maximum values during vibration were calculated by assuming a zero value at the start of each excitation step. Figure 7 shows the accumulated residual values for the differences between the stresses of the left and right pressure receiving plates at different vibration steps. Similarly, Figure 8 shows the accumulated residual values of the horizontal displacements of the building model and ground at different vibration steps, and Figure 9 shows the accumulated residual values of the displacements measured by the relative displacement gauge at different vibration steps. These figures confirm that the residual values rapidly increased after vibration step d09.

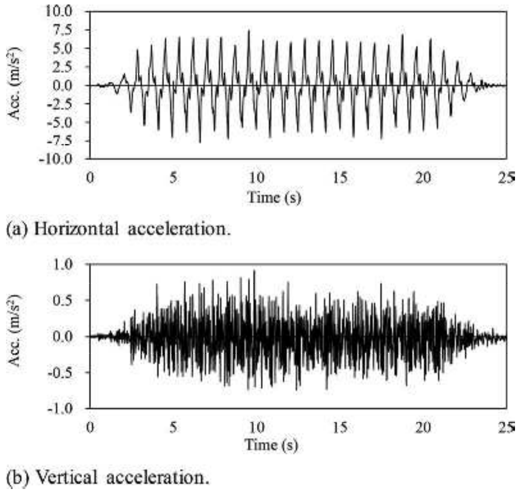

Figure 5. Input acceleration (vibration step d04).

Table 2. Maximum values of the acceleration amplitude at different vibration steps.

Vibration step	Frequency	Horizontal acc. m/s^2	Vertical acc. m/s^2
d01	1.2	0.57	0.13
d02	1.2	3.47	0.42
d03	1.2	5.72	1.15
d04	1.2	7.77	0.91
d05	1.2	9.16	1.22
d06	1.2	10.40	1.50
d07	1.6	8.68	1.87
d08	1.6	10.04	2.88
d09	1.6	11.53	3.84
d10	1.6	11.25	3.39

Figure 10 shows the strain distribution calculated from images captured by a high-speed camera at vibration step d10. Cracks connecting the lower end of the weak layer and the left side of the building model were generated, although they were not yet clear in images captured at vibration step d09. Owing to the occurrence of these cracks, the upper part of the weak layer was estimated to move.

3 EVALUATION OF THE SLIP SAFETY FACTOR

The results of the dynamic centrifugal model test were used to evaluate the applicability of the slip safety factor evaluation method based on the equivalent linear analysis. The properties of the rock foundation model used for the equivalent linear analysis are listed in Table 1. The dynamic deformation characteristics of the artificial rock material were set (Figure 3) by using the general hyperbolic equation (GHE) model (Tatsuoka & Shibuya 1992). In contrast, the artificial weak layer was modeled to represent linear elastic-joint elements. The unit weight of

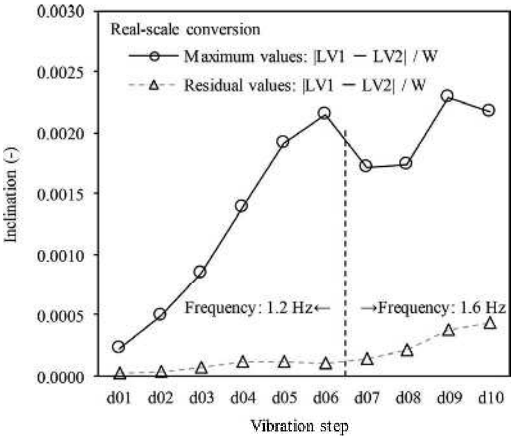

Figure 6. Maximum and accumulated residual values for the inclination of the building model at different vibration steps.

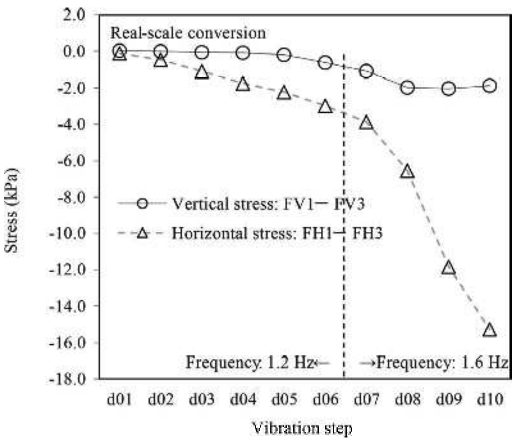

Figure 7. Accumulated residual values for the difference in stresses at different vibration steps.

the artificial weak layer was 20.6 kN/m^3, which was equal to that of the Teflon sheet, and the corresponding Poisson's ratio was 0.49 based on the assumption of no volume change. The pseudo shear modulus of elasticity, which was induced by modeling the artificial weak layer as linear elastic-joint elements, was set as 2800 kN/m^2 from the gradient up to the maximum shear resistance during the single-plane shearing tests.

Equivalent linear analyses were performed with the same input accelerogram as that measured in the centrifugal model test. The stresses used to calculate the slip safety factor were obtained by adding the stresses from the self-weight stresses and induced during an earthquake. Figure 11 shows the procedure for calculating the slip safety factor.

Table 3 lists the minimum slip safety factor values calculated during the different vibration steps, and Figure 12 shows the slip-line shapes

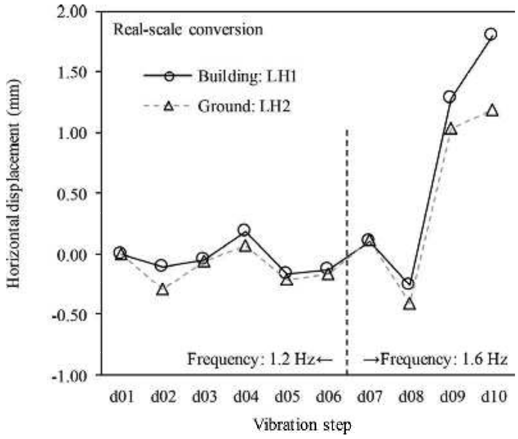

Figure 8. Accumulated residual values for the horizontal dis-placements of the building model and ground at different vi-bration steps.

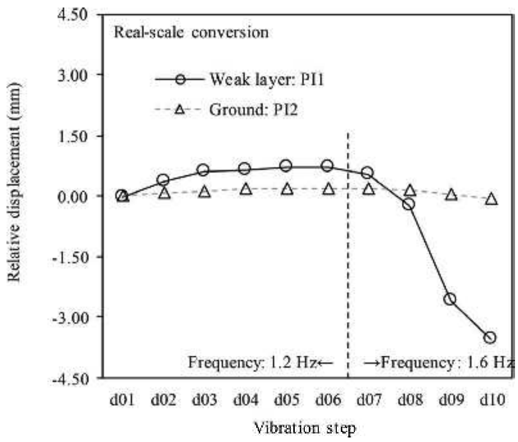

Figure 9. Accumulated residual values for the displacements obtained by the relative displacement gauge at different vibra-tion steps.

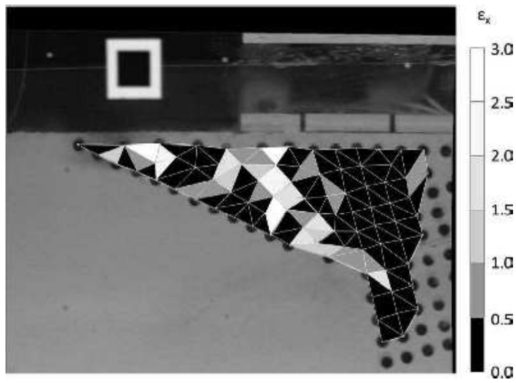

Figure 10. Horizontal strain distribution calculated from im-ages taken with a high-speed camera at vibration step d10.

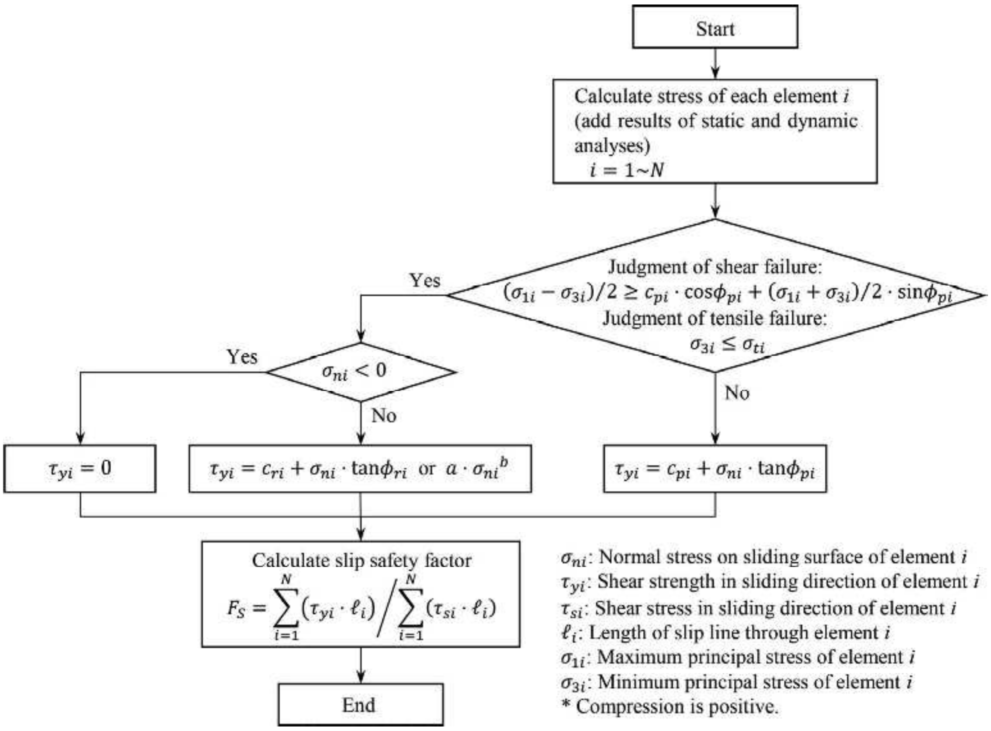

Figure 11. Flowchart for calculating the slip safety factor.

Table 3. Slip safety factors for different vibration steps.

Vibration step	Minimum slip safety factor		Slip safety factor obtained from model test	
	Slip line		Slip line	
d01	No. 6	24.78		24.78
d02	No. 6	8.38		8.38
d03	No. 5	5.10		5.61
d04	No. 4	3.02		3.33
d05	No. 1	2.12	No. 6	2.67
d06	No. 6	1.40		1.40
d07	No. 6	1.76		1.76
d08	No. 3	0.86		0.98
d09	No. 2	0.39		0.72
d10	No. 2	0.20		0.45

corresponding to these values. The minimum slip safety factor was less than 1 after vibration step d08, although the residual displacement rapidly increased at vibration step d09 during the test. Therefore, the slip safety factor evaluation method can be considered conservative. Although the slip safety factor of the slip line generated during the tests does not represent the minimum value, it is similar in that it was less than 1 before the residual displacement rapidly increased. In addition, even when the slip safety factor was less than 1, the amount of displacement that could be caused by sliding was limited. This indicates that, in the event of an earthquake, rock foundations do not spontaneously lose their seismic stability.

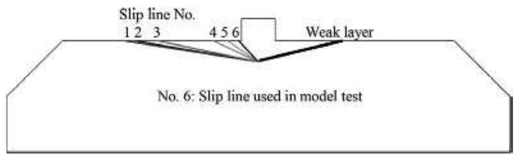

Figure 12. Slip line shapes for the minimum slip safety factor.

4 CENTRIFUGAL MODEL TEST ASSUMING SLIDING FROM THE BEGINNING

In the centrifugal model test described above, even when the slip safety factor was less than 1, the amount of displacement due to sliding was limited, and the rock foundation did not become rapidly unstable. In order to confirm this more clearly, a centrifugal model test was performed assuming the occurrence of slip clump under the building model, as shown in Figure 13. Although only the surroundings of the building model are shown in this figure, the other model shapes and instrument arrangement were the same as that in Figure 1. The slip clump and weak layers were made of the same artificial rock material and Teflon sheets as above.

Table 4 lists the maximum accelerations measured at the bottom of the rock foundation model and the minimum slip safety factors at different vibration steps. Figure 14 shows the maximum

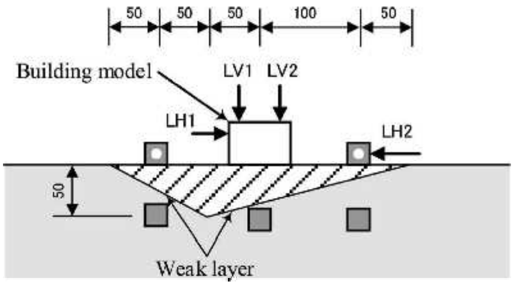

Figure 13. Rock foundation model for the centrifugal model test assuming the occurrence of slip clump under the building model.

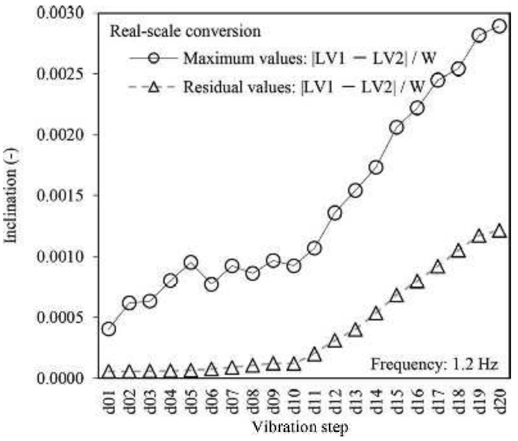

Figure 14. Maximum and accumulated residual values for the inclination of the building model at different vibration steps.

values during vibration and the accumulated residual values for the inclination of the building model at different vibration steps. The results once again confirmed that, even when the slip safety factor was less than 1, the rock foundation did not become unstable spontaneously.

5 CONCLUSION

The centrifugal model tests in this study confirmed the feasibility of the slip safety factor evaluation method. In addition, the displacement of rock masses because of sliding was observed to be limited even when the slip safety factor was less than 1. This confirms that, in the event of an earthquake, rock foundations do not become unstable spontaneously. Therefore, evaluating the seismic stability based on ground displacement is considered to be an effective approach.

Table 4. Maximum accelerations measured at the bottom of the rock foundation model and minimum slip safety factors at dif-ferent vibration steps.

Vibration step	Frequency	Horizontal acc. m/s^2	Vertical acc. m/s^2	Minimum slip safety factor
d01		0.39	0.09	1.85
d02		1.29	0.29	0.59
d03		1.81	0.38	0.41
d04		2.01	0.51	0.25
d05		2.46	0.72	0.19
d06		2.47	0.44	0.19
d07		2.86	0.63	0.19
d08		3.39	0.57	0.17
d09		4.07	0.87	0.14
d10	1.2	4.61	0.80	0.14
d11		5.09	0.89	0.14
d12		5.64	0.84	0.15
d13		5.92	1.02	0.12
d14		6.24	1.09	0.12
d15		6.53	1.17	0.11
d16		7.41	1.12	0.10
d17		7.79	1.26	0.09
d18		8.10	1.37	0.10
d19		8.79	1.65	0.09
d20		9.54	1.26	0.10

6 ACKNOWLEDGMENTS

This work is part of a collaborative research project that was carried out jointly by Kansai Electric Power Co. Inc., Hokkaido Electric Power Co. Inc., Tohoku Electric Power Co. Inc., Tokyo Electric Power Company Holdings, Inc., Chubu Electric Power Co. Inc., Hokuriku Electric Power Co. Inc., Chugoku Electric Power Co. Inc., Shikoku Electric Power Co. Inc., Kyusyu Electric Power Co. Inc., The Japan Atomic Power Company, Electric Power Development Co., Ltd., and Japan Nuclear Fuel Limited.

REFERENCES

Ishimaru, M. and Kawai, T. 2011. Centrifuge model test on earthquake-induced failure behaviour of slope in discontinuous rock mass. *Proc. 12th International Congress on Rock Mechanics*, Beijing: 1919–1922.

JEAG4601-1987. 1987. Technical Guidelines for Aseismic Design of Nuclear Power Plants, Japan.

Tatsuoka, F. and Shibuya, S. 1992. Deformation characteristics of soils and rocks from field and laboratory tests. *Proc. 9th Asian Regional Conference on Soil Mechanics and Foundation Engineering*, Bangkok, Vol. 2: 101–170.